

The missing link: discerning true from false negatives when sampling species interaction networks

[Michael D. Catchen](#)^{1,2} [Timothée Poisot](#)^{3,2} [Laura Pollock](#)^{1,2} [Andrew Gonzalez](#)^{1,4}

¹ McGill University ² Québec Centre for Biodiversity Sciences ³ Université de Montréal ⁴ Québec Centre for Biodiversity Science

Correspondance to:

Michael D. Catchen — michael.catchen@mcgill.ca

Abstract: Ecosystems are composed of networks of interacting species. These interactions allow communities of species to persist through time through both neutral and adaptive processes. Still a robust understanding of (and ability to predict and forecast) interactions among species remains elusive. This knowledge-gap is largely driven by a shortfall of data—although species occurrence data has rapidly increased in the last decade, species interaction data has not kept pace, largely due to the intrinsic difficulty and effort required to sample interactions. These sampling challenges bias data and hinder inferences about the structure and dynamics of interactions networks. Here, we demonstrate the realized false-negative rate (the percentage of species that actually interact but for which we do not yet have a record) can be quite high, even in thoroughly sampled systems, due to the intrinsic variation in abundances across species in a community. We illustrate how a null model of occurrence detection can be used to estimate the false-negative rate in a given dataset. We also show how to directly incorporate uncertainty due to observation error into model-based predictions of interaction probabilities between species. One hypothesis is that interactions between “rare” species are themselves rare because these species are less likely to encounter one-another than species of higher relative abundance. However, we demonstrate that across several datasets of spatial or temporally replicated networks, there are positive associations that suggest these interactions actually exist but just are not observed. Finally, we assess how false negatives influence various models of network prediction, and recommend directly accounting for observation error in predictive models. We conclude by discussing how the understanding of false-negatives can inform how we design monitoring schemes for species interactions.

1 Introduction

2 Species interactions drive many processes in evolution and ecology. A better understanding of species
3 interactions is an imperative to understand the evolution of life on Earth, to mitigate the impacts of
4 anthropogenic change on biodiversity (Makiola *et al.* 2020), and for predicting zoonotic spillover of
5 disease to prevent future pandemics (Becker *et al.* 2021). At the moment we lack sufficient data to meet
6 these challenges (Poisot *et al.* 2021), largely because species interactions are hard to sample (Jordano
7 2016). Over the past few decades biodiversity data has become increasingly available through remotely
8 collected data and adoption of open data practices (Kenall *et al.* 2014; Stephenson 2020). Still, interaction
9 data remains relatively scarce because sampling typically requires human observation. This induces a
10 constraint on the amount, spatial scale, and temporal frequency of resulting data that it is feasible to
11 collect by humans. Many crowdsourced methods for biodiversity data aggregation (e.g. GBIF, eBird) still
12 relies on automated identification of species, which does not easily generalize to interaction sampling.
13 There is interest in using remote methods for interaction sampling, which primarily detect co-occurrence
14 and derive properties like species avoidance from this data (Niedballa *et al.* 2019). However, this itself is
15 not necessarily indicative of an interaction (Blanchet *et al.* 2020). This is an example of semantic
16 confusion around the word “interaction”—for example one might consider competition a type of species
17 interaction, even though it is marked by a lack of co-occurrence between species, unlike other types of
18 interactions, like trophism or pollination, which require both species to be together at the same place and
19 time. Here we consider interaction in the latter sense, where two species have fitness consequences on
20 one-another if (and only if) they are in the sample place at the same time. In addition, here we only
21 consider direct (not higher-order) interactions.

22 We cannot feasibly observe all (or even most) of the interactions that occur in an ecosystem. This means
23 we can be confident two species actually interact if we have a record of it (given an estimate of species
24 misidentification probability), but not at all confident that a pair of species *do not* interact if we have *no*
25 *record* of those species observed together. In other words, it is difficult to distinguish *true-negatives* (two
26 species never interact) from *false-negatives* (two species interact sometimes, but we do not have a record of
27 it). For a concrete example of a false-negative in a food web, see fig. 1. Because even the most highly
28 sampled systems will still contain missing interactions, there is increasing interest in combining
29 species-level data (e.g. traits, abundance, range, phylogenetic relatedness, etc.) to build models to predict

30 interactions between species we haven't observed together before (Strydom *et al.* 2021). However, the
31 noise of false-negatives could impact the efficacy of our predictive models and have practical
32 consequences for answering questions about interactions (de Aguiar *et al.* 2019). This data constraint is
33 amplified as the interaction data we have is geographically biased toward the usual suspects (Poisot *et al.*
34 2021). We therefore need a statistical approach to assessing these biases in the observation process and
35 their consequences for our understanding of interaction networks.

36 The importance of *sampling effort* and its impact on resulting ecological data has produced a rich body of
37 literature. The recorded number of species in a dataset or sample depends on the total number of
38 observations (Walther *et al.* 1995; Willott 2001), as do estimates of population abundance (Griffiths 1998).
39 This relationship between sampling effort and spatial coverage and species detectability. This has
40 motivated more quantitatively robust approaches to account for error in sampling data in many contexts:
41 to determine if a given species is extinct (Boakes *et al.* 2015), to determine sampling design (Moore &
42 McCarthy 2016), and to measure species richness across large scales (Carlson *et al.* 2020). In the context of
43 interactions, an initial concern was the compounding effects of limited sampling effort combined with the
44 amalgamation of data (across both study sites, time of year, and taxonomic scales) could lead any
45 empirical set of observations to inadequately reflect the reality of how species interact (Paine 1988) or the
46 structure of the network as a whole (Martinez *et al.* 1999; McLeod *et al.* 2021). Martinez *et al.* (1999)
47 showed that in a plant-endophyte trophic network, network connectance is robust to sampling effort, but
48 this was done in the context of a system for which observation of 62,000 total interactions derived from
49 164,000 plant-stems was feasible. In some systems (e.g. megafauna food-webs) this many observations is
50 either impractical or infeasible due to the absolute abundance of the species in question.

51 The intrinsic properties of ecological communities create several challenges for sampling: first, species are
52 not observed with equal probability—we are much more likely to observe a species of high abundance
53 than one of very low abundance (Poisot *et al.* 2015). Canard *et al.* (2012) presents a null model of food-web
54 structure where species encounter one-another in proportion to each species' relative-abundance. This
55 assumes that there are no associations in species co-occurrence due to an interaction (perhaps because
56 this interaction is “important” for both species; Cazelles *et al.* (2016)), but in this paper we later show
57 increasing strength of associations leads to increasing probability of false-negatives in interaction data,
58 and that these positive associations are rampant in existing network data. Second, observed co-occurrence
59 is often equated with meaningful interaction strength, but this is not necessarily the case (Blanchet *et al.*

2020)—a true “non-interaction” would require that neither of two species, regardless of whether they co-occur, ever exhibit any meaningful effect on the fitness of the other. So, although co-occurrence is not directly indicative of an interaction, it is a precondition for an interaction.

Here, we illustrate how our confidence that a pair of species never interacts highly depends on sampling effort. We suggest that surveys of species interactions can benefit from simulation modeling of the sampling process. We demonstrate how the realized false-negative rate of interactions is related to the relative abundance of the species pool, and use simulation to produce a null estimate of the false-negative rate given total sampling effort (the total count of all individuals of all species seen), and to introduce a method for introducing uncertainty into model predictions of interaction probability to account for observation error. We then show that positive associations in co-occurrence data can increase the realized number of false-negatives, and demonstrate these positive associations are rampant in network datasets, and conclude by recommending that the simulation of sampling effort and species occurrence can and should be used to help design surveys of species interaction diversity (Moore & McCarthy 2016), and by advocating use of null models like those presented here as a tool for both guiding design of surveys of species interactions and for modeling detection error in predictive models.

[Figure 1 about here.]

Accounting for false-negatives in species interactions

How many observations of a non-interaction do we need to be confident it's a true negative?

We start with a naive model of interaction detection: we assume that every interacting pair of species is incorrectly observed as not-interacting with an independent and fixed probability, which we denote p_{fn} and subsequently refer to as the False-Negative Rate (FNR). If we observe the same species not-interacting N times, then the probability of a true-negative (denoted p_{tn}) is given by $p_{tn} = 1 - (p_{fn})^N$. This relation (the probability-mass-function of geometric distribution, a special case of the negative-binomial distribution) is shown in fig. 2(A) for varying values of p_{fn} and illustrates a fundamental link between our ability to reliably say an interaction doesn't exist— p_{tn} —and the number of times N we have observed a

86 given species. In addition, note that there is no non-zero p_{fn} for which we can ever *prove* that an
87 interaction does not exist—no matter how many observations of non-interactions N we have, $p_{tn} < 1$.
88 From fig. 2(A) it is clear that the more often we see two species co-occurring, but *not interacting*, the more
89 likely the interaction is a true-negative. This has several practical consequences: first it means negatives
90 taken outside the overlap of the range of each species aren't informative because co-occurrence was not
91 possible, and therefore neither was an interaction. Second, we can use this relation to compute the
92 expected number of total observations needed to obtain a “goal” number of observations of a particular
93 pair of species (fig. 2(B)). As an example, if we hypothesize that A and B do not interact, and we want to see
94 species A and B both co-occurring and *not interacting* 10 times to be confident this is a true negative, then
95 we need an expected 1000 observations of all species if the relative abundances of A and B are both 0.1.
96 Because the true FNR is latent, we can never actually be sure what the actual number of false negatives in
97 our data—however, we can use simulation to estimate it for datasets of a given size using neutral models
98 of observation. If some of the “worst-case” FNRs presented in fig. 2(A) seem unrealistically high, consider
99 that species are observed in proportion to their relative abundance. In the next section we demonstrate
100 that the distribution of abundance in ecosystems can lead to very high realized values of FNR (p_{fn}) simply
101 as an artifact of sampling effort.

102 [Figure 2 about here.]

103 **False-negatives as a product of relative abundance**

104 We now show that the realized FNR changes drastically with sampling effort due to the intrinsic variation
105 of the abundance of individuals of each species within a community. We do this by simulating the process
106 of observation of species interactions, applied both to 243 empirical food webs from the Mangal database
107 (Banville *et al.* 2021) and random food-webs generated using the niche model, a simple generative model
108 of food-web structure that accounts for allometric scaling (Williams & Martinez 2000). Our neutral model
109 of observation assumes each observed species is drawn in proportion to each species' abundance at that
110 place and time. The abundance distribution of a community can be reasonably-well described by a
111 log-normal distribution (Volkov *et al.* 2003). In addition to the log-normal distribution, we also tested the
112 case where the abundance distribution is derived from power-law scaling $Z^{(\log(T_i)-1)}$ where T_i is the
113 trophic level of species i and Z is a scaling coefficient (Savage *et al.* 2004), which yields the same

114 qualitative behavior. The practical consequence of abundance distributions spanning many orders of
115 magnitude of abundance is that observing two “rare” species interacting requires two low probability
116 events: observing two rare species *at the same time*.

117 To simulate the process of observation, for an ecological network M with S species, we sample abundances
118 for each species from a standard-log-normal distribution. For each true interaction in the adjacency matrix
119 M (i.e. $M_{ij} = 1$) we estimate the probability of observing both species i and j at a given place and time by
120 simulating n observations of all individuals of any a species, where the species of the individual observed
121 at the $\{1, 2, \dots, n\}$ -th observation is drawn from the generated log-normal distribution of abundances. For
122 each pair of species (i, j) , if both i and j are observed within the n -observations, the interaction is tallied as
123 a true positive if $M_{ij} = 1$. If only one of i or j are observed—but not both—in these n observations, but
124 $M_{ij} = 1$, this is counted as a false-negative, and a true-negative otherwise. For each pair of species (i, j) , if
125 both i and j are observed within the n -observations, the interaction is tallied as a true positive if $M_{ij} = 1$.
126 If only one of i or j are observed—but not both—in these n observations, but $M_{ij} = 1$, this is counted as a
127 false-negative, and a true-negative otherwise ($M_{ij} = 0$). This process is illustrated conceptually in fig. 3(A).
128 In fig. 2(C) we see this model of observation applied to niche model networks across varying levels of
129 species richness, and in fig. 2(D) the observation model applied to Mangal food webs. For all niche model
130 simulations in this manuscript, for a given number of species S the number of interactions is drawn from
131 the flexible-links model fit to Mangal data (MacDonald *et al.* 2020), effectively drawing the number of
132 interactions L for a random niche model food-web as

$$L \sim \text{BetaBinomial}(S^2 - S + 1, \mu\phi, 1 - \mu\phi)$$

133 where the MAP estimate of (μ, ϕ) applied to Mangal data from (MacDonald *et al.* 2020) is
134 ($\mu = 0.086$, $\phi = 24.3$). All simulations were done with 500 independent replicates of unique niche model
135 networks per unique number of observations n . All analyses presented here are done in Julia v1.8
136 (Bezanson *et al.* 2015) using both EcologicalNetworks.jl v0.5 and Mangal.jl v0.4 (Banville *et al.* 2021) and
137 are hosted on [Github](#)). Note that the empirical data, for the reasons described above, very likely already
138 contains many false negatives, we’ll revisit this issue in the final section.

139 From fig. 2(C) it is evident that the number of species considered in a study is inseparable from the
140 false-negative rate in that study, and this effect should be taken into account when designing samples of

ecological networks in the future. We see a similar qualitative pattern in fig. 2(D) where the FNR drops off quickly as a function of observation effort, mediated by total richness. The practical consequence of the bottom row of fig. 2 is whether the total number of observations of all species (the x-axis) for the threshold FNR we deem acceptable (the y-axis) is feasible. This raises two points: first, empirical data on interactions are subject to the practical limitations of funding and human-work hours, and therefore existing data tend to fall on the order of hundreds or thousands observations of individuals per site. Clear aggregation of data on sampling effort has proven difficult to find and a meta-analysis of network data and sampling effort seems both pertinent and necessary, in addition to the effects of aggregation of interactions across taxonomic scales (Gauzens *et al.* 2013; Giacomuzzo & Jordán 2021). This inherent limitation on in-situ sampling means we should optimize where we sample across space so that for a given number of samples, we obtain the maximum information possible. Second, what is meant by “acceptable” FNR? This raises the question: does a shifting FNR lead to rapid transitions in our ability inference and predictions about the structure and dynamics of networks, or does it produce a roughly linear decay in model efficacy? We explore this in the next section.

We conclude this section by advocating for the use of neutral models similar to above to generate expectations about the number of false-negatives in a data set of a given size. This could prove fruitful both for designing surveys of interactions but also because we may want to incorporate models of imperfect detection error into predictive interactions models, as Joseph (2020) does for species occurrence modeling. Additionally, we emphasize that one must consider the context for sampling—is the goal to detect a particular species (as in fig. 2(C)), or to get a representative sample of interactions across the species pool? These arguments are well-considered when sampling individual species (Willott 2001), but have not yet been adopted for designing samples of communities.

Including observation error in interaction predictions

Here we show how to incorporate uncertainty into model predictions of interaction probability to account for imperfect observation (both false-negatives and false-positives). Models for interaction prediction typically yield a probability of interaction between each pair of species, p_{ij} . When these are considered with uncertainty, it is usually model-uncertainty, e.g. the variance in the interaction probability prediction across several cross-validation folds, where the data is split into training and test sets several times. The method we introduce adjusts the value of a model’s predictions to produce a distribution of interaction

probabilities, which are adjusted by a given false-negative-rate p_{fn} and false-positive-rate p_{fp} (outlined in figure fig. 3). We describe first how to sample from this distribution of adjusted interaction probabilities via simulation, and show that this distribution can be well-approximated analytically.

[Figure 3 about here.]

We then consider the output prediction from an arbitrary prediction model, which is the probability p_{ij} that two species i and j interact. To get an estimate of p_{ij} that accounts for observation error, we resample the probability of each interaction p_{ij} by simulating a set of several ‘particles,’ where each particle is a realization of an interaction occurring (either true or false with probabilities p_{ij} and $1 - p_{ij}$ respectively) and then being correctly observed with probabilities given by p_{fp} and p_{fn} to yield a single boolean outcome for each particle. (“Resampling” within fig. 3 (B)). Over many samples of particles, the resulting frequency of ‘true’ outcomes is a single resample of the interaction probability p_{ij}^* . Across several samples each of several particles, this forms a distribution of probabilities which are adjusted by the true and false negative rates.

There is also an analytic way to approximate this distribution using the normal approximation to binomial. As a reminder, as the total number of samples n from a binomial distribution with success probability p from approaches infinity, the sum of total successes across all samples approaches a normal distribution with mean np and variance $np(1 - p)$. We can use this to correct the estimate p_{ij} based on the expected false-negative-rate p_{fn} and false-positive rate p_{fp} to obtain the limiting distribution as the number of resamples approaches infinity for the resampled p_{ij}^* for a given number of particles n_p . We do this by first adjusting for the rates of observation error to get the mean resampled probability, $\mathbb{E}[p_{ij}^*]$, as

$$\mathbb{E}[p_{ij}^*] = p_{ij}(1 - p_{fp}) + (1 - p_{ij})p_{fn}$$

which yields the normal approximation

$$\sum_{i=1}^{n_p} p_{ij}^* \sim \mathcal{N}\left(n_p \cdot \mathbb{E}[p_{ij}^*], \sqrt{n_p \mathbb{E}[p_{ij}^*](1 - \mathbb{E}[p_{ij}^*])}\right)$$

which then can be converted back to a distribution of frequency of successes to yield the final approximation

$$p_{ij}^* \sim \mathcal{N}\left(\mathbb{E}[p_{ij}^*], \sqrt{\frac{\mathbb{E}[p_{ij}^*](1 - \mathbb{E}[p_{ij}^*])}{n_p}}\right) \quad (1)$$

We can then further truncate to remain on the interval (0, 1) (as the output is a probability, although in practice often the probability mass outside (0, 1) is extremely low. As an example case study, we use a boosted-regression-tree to predict interactions in a host-parasite network (Hadfield *et al.* 2014) (with features derived in the same manner as Strydom *et al.* (2021) derives features on this data) to produce a set of interaction predictions. We then applied this method to a set of a few resampled interaction probabilities between mammals and parasite species shown in figure fig. 3(C).

Why is this useful? For one, this analytic method avoids the extra computation required by simulating samples from this distribution directly. Further, it enables continuous examination of the number of particles n_p as a uncertainty width. The natural analogue for the number of particles sampled is the number of observations of co-occurrence for a given pair of species—the fewer the particles, the higher the variance of the resulting approximation (see supplemental figure 1 for an example). Equation (ref:eq:eq1?) is undefined for 0 particles (i.e. 0 observations co-occurrence), although as n_p approaches 0 the approxated normal (once truncated) approaches a uniform distribution on the interval (0, 1), the maximum entropy distribution where we have no information about the possibility of an interaction.

This also has implications for what we mean by ‘uncertainty’ in interaction predictions. A model’s prediction can be ‘uncertain’ in two different ways: (1) the model’s predictions may have high variance, or (2) the model’s predictions may be centered around a probability of interaction of 0.5, where we are the most unsure about whether this interaction exists. For non-zero p_{fn} and p_{fp} , the above model always moves the mean interaction probability toward 0.5 (supplemental figure 2), siding toward higher uncertainty in the latter (higher entropy) sense. Improving the incorporation of different forms of uncertainty in probabilistic interaction predictions seems a necessary next step toward understanding what pairs of species we know the least about, in order to prioritize sampling to provide the most new information possible.

Positive associations in co-occurrence increase the false-negative rate

The model above doesn't consider the possibility that there are positive or negative associations which shift the probability of species cooccurrence together due to their interaction (Cazelles *et al.* 2016). However, here we demonstrate that the probability of observing a false-negative can be higher if there is some positive association in the occurrence of species A and B . If we denote the probability that we observe the co-occurrence of two species A and B as $P(AB)$ and if there is no association between the marginal probabilities of observing A and observing B , denoted $P(A)$ and $P(B)$ respectively, then the probability of observing their co-occurrence is the product of the marginal probabilities for each species, $P(AB) = P(A)P(B)$. In the other case where there is some positive strength of association between observing both A and B because this interaction is "important" for each species, then the probability of observation both A and B , $P(AB)$, is greater than $P(A)P(B)$ as $P(A)$ and $P(B)$ are not independent and instead are positively correlated, i.e. $P(AB) > P(A)P(B)$. In this case, the probability of observing a single false-negative in our naive model from fig. 2(A) is $p_{fn} = 1 - P(AB)$, which due to the above inequality implies $p_{fn} > 1 - P(A)P(B)$. This indicates an increasingly greater probability of a false negative as the strength of association gets stronger, $P(AB) \rightarrow P(AB) \gg P(A)P(B)$. However, this still does not consider variation in species abundance in space and time (Poisot *et al.* 2015). If positive or negative associations between species structure variation in the distribution of $P(AB)$ across space/time, then the spatial/temporal biases induced by data collection would further impact the realized false negative rate, as the probability of false negative would not be constant for each pair of species across sites.

To test for these positive associations in data we scoured Mangal for datasets with many spatial or temporal replicates of the same system. For each dataset, we compute the marginal probability $P(A)$ of occurrence of each species A across all networks in the dataset. For each pair of interacting species A and B , we then compute and compare the probability of co-occurrence if each species occurs independently, $P(A)P(B)$, to the empirical joint probability of co-occurrence, $P(AB)$. Following our analysis above, if $P(AB)$ is greater than $P(A)P(B)$, then we expect our neutral estimates of the FNR above to underestimate the realized FNR. In fig. 4, we see the difference between $P(AB)$ and $P(A)P(B)$ for the seven suitable datasets with enough spatio-temporal replicates and a shared taxonomic backbone (meaning all individual networks use common species identifiers) found on Mangal to perform this analysis. Further details about each dataset are reported in tbl. 1.

In each of these datasets, the joint probability of co-occurrence $P(AB)$ is decisively greater than our expectation if species co-occur in proportion to their relative abundance $P(A)P(B)$. This suggests that there may not be as many “neutrally forbidden links” (Canard *et al.* 2012) as we might think, and that the reason we do not have records of interactions between rare species is probably due to observation error. This has serious ramifications for the widely observed property of nestedness seen in bipartite networks (Bascompte & Jordano 2007)—perhaps the reason we have lots of observations between generalists is because they are more abundant, and this is particularly relevant as we have strong evidence that generalism drives abundance (Song *et al.* 2022a), not vice-versa.

[Figure 4 about here.]

Table 1: This table describes the datasets used in the above analysis (Fig 2). The table reports the type of each dataset, the total number of networks in each dataset (N), the total species richness in each dataset (S), the connectance of each metaweb (all interactions across the entire spatial-temporal extent) (C), the mean species richness across each local network \bar{S} , the mean connectance of each local network \bar{C} , the mean β -diversity among overlapping species across all pairs of network species ($\bar{\beta}_{OS}$), and the mean β -diversity among all species in the metaweb ($\bar{\beta}_{WN}$). Both metrics are computed using KGL β -diversity (Koleff *et al.* 2003)

Network	Type	N	S	C	\bar{S}	\bar{C}	$\bar{\beta}_{OS}$	$\bar{\beta}_{WN}$
Kopelke <i>et al.</i> (2017)	Food Web	100	98	0.037	7.87	0.142	1.383	1.972
Thompson & Townsend (2000)	Food Web	18	566	0.014	80.67	0.049	1.617	1.594
Havens (1992)	Food Web	50	188	0.065	33.58	0.099	1.468	1.881
Ponisio <i>et al.</i> (2017)	Pollinator	100	226	0.079	23.0	0.056	1.436	1.870
Hadfield <i>et al.</i> (2014)	Host-Parasite	51	327	0.085	32.71	0.337	1.477	1.952
Closs & Lake (1994)	Food Web	12	61	0.14	29.09	0.080	1.736	1.864
CaraDonna <i>et al.</i> (2017)	Pollinator	86	122	0.18	21.42	0.312	1.527	1.907

The impact of false-negatives on network properties and prediction

Here, we assess the effect of false negatives on our ability to make predictions about interactions, as well as their effect on network structure. The prevalence of false-negatives in data is the catalyst for interaction prediction in the first place, and as a result methods have been proposed to counteract this bias (Stock *et*

258 *al.* 2017; Poisot *et al.* 2022). However, it is feasible that the FNR in a given dataset is so high that it could
259 induce too much noise for an interaction prediction model to detect the signal of possible interaction
260 between species.

261 To test this we use the dataset from Hadfield *et al.* (2014) that describes host-parasite interaction networks
262 sampled across 51 sites, and the same method as Strydom *et al.* (2021) to extract latent features for each
263 species in this dataset based on applying PCA to the co-occurrence matrix. We then predict a metaweb
264 (equivalent to predicting true or false for an interaction between each species pair, effectively a binary
265 classification problem) from these species-level features using four candidate models for binary
266 classification—three often used machine-learning (ML) methods (Boosted Regression Tree (BRT),
267 Random Forest (RF), Decision Tree (DT)), and one naive model from classic statistics (Logistic Regression
268 (LR)). Each of the ML models are bootstrap aggregated (or bagged) with 100 replicates each. We partition
269 the data into 80-20 training-test split, and then seed the training data with false negatives at varying rates,
270 but crucially do nothing to the test data. We fit all of these models using MLJ.jl, a high-level Julia
271 framework for a wide-variety of ML models (Blaom *et al.* 2020). We evaluate the efficacy of these models
272 using two common measures of binary classifier performance: the area under the receiver-operator curve
273 (ROC-AUC) and the area under the precision-recall curve (PR-AUC), for more details see Poisot (2022).
274 Here, PR-AUC is slightly more relevant as it is a better indicator of prediction of false-negatives. The
275 results of these simulations are shown in fig. 5(A&B).

276 [Figure 5 about here.]

277 One interesting result seen in fig. 5(A&B) is that the ROC-AUC value does not approach random in the
278 same way the PR-AUC curve does as we increase the added FNR. The reason for this is that ROC-AUC is
279 fundamentally not as useful a metric in assessing predictive capacity as PR-AUC. As we keep adding more
280 false-negatives, the network eventually becomes a zeros matrix, and these models can still learn to predict
281 “no-interaction” for all possible species pairs, which does far better than random guessing (ROC-AUC =
282 0.5) in terms the false positive rate (one of the components of ROC-AUC). This highlights a more broad
283 issue of label class imbalance, meaning there are far more non-interactions than interactions in data. A
284 full treatment of the importance of class-balance is outside the scope of this paper, but is explored in-depth
285 in Poisot (2022).

286 Although these ML models are surprisingly performant at link prediction given their simplicity, there

287 have been several major developments in applying deep-learning methods to many tasks in network
288 inference and prediction—namely graph-representation learning (GRL, Khoshraftar & An (2022)) and
289 graph convolutional networks (Zhang *et al.* 2019). At this time, these advances can not yet be applied to
290 ecological networks because they require far more data than we currently have. We already have lots of
291 features that could be used as inputs into these models (i.e. species level data about occurrence, genomes,
292 abundance, etc.), but our network datasets barely get into the hundreds of local networks sampled across
293 space and time (tbl. 1). Once we start to get into the thousands, these models will become more useful, but
294 this can only be done with systematic monitoring of interactions. This again highlights the need to
295 optimize our sampling effort to maximize the amount of information contained in our data given the
296 expensive nature of sampling interactions.

297 We also consider how the FNR affects network properties. In fig. 5(C) we see the mean trophic level across
298 networks simulated using the niche model (as above), across a spectrum of FNR values. In addition to the
299 clear dependence on richness, we see that mean trophic level, despite varying widely between niche model
300 simulations, tends to be relatively robust to false negatives and does not deviate widely from the true value
301 until very large FNRs, i.e. $p_{fn} > 0.7$. This is not entirely unsurprising. Removing links randomly from a
302 food-web is effectively the inverse problem of the emergence of a giant component (more than half of the
303 nodes are in a connected network) in random graphs (see Li *et al.* (2021) for a thorough review). The
304 primary difference being that we are removing edges, not adding them, and thus we are witnessing the
305 dissolution of a giant component, rather than the emergence of one. Further applications of percolation
306 theory to the topology of ecological networks could improve our understanding of how false-negatives
307 impact the inferences about the structure and dynamics on these networks.

308 Discussion

309 Species interactions enable the persistence and functioning of ecosystems, but our understanding of
310 interactions is limited due to the intrinsic difficulty of sampling. Here we have provided a null model for
311 the expected number of false-negatives in an interaction dataset. We demonstrated that we expect many
312 false-negatives in species interaction datasets purely due to the intrinsic variation of abundances within a
313 community. We also, for the first time to our knowledge, measured the strength of association between
314 co-occurrence and interactions (Cazelles *et al.* 2016) across many empirical systems, and found that these

315 positive associations are both very common, and showed algebraically that they increase the realized FNR.
316 We have also shown that false-negatives could further impact our ability to both predict interactions and
317 infer properties of the networks, which highlights the need for further research into methods for
318 correcting this bias in existing data.

319 A better understanding of how false-negatives impact species interaction data is a practical
320 necessity—both for inference of network structure and dynamics, but also for prediction of interactions by
321 using species level information. False-negatives could pose a problem for many forms of inference in
322 network ecology. For example, inferring the dynamic stability of a network could be prone to error if the
323 observed network is not sampled “enough.” What exactly “enough” means is then specific to the
324 application, and should be assessed via methods like those here when designing samples. Further,
325 predictions about network rewiring (Thompson & Gonzalez 2017) due to range shifts in response to
326 climate change could be error-prone without accounting for interactions that have not been observed but
327 that still may become climatically infeasible. As is evident from fig. 2(A), we can never guarantee there are
328 no false-negatives in data. In recent years, there has been interest toward explicitly accounting for
329 false-negatives in models (Stock *et al.* 2017; Young *et al.* 2021), and a predictive approach to
330 networks—rather than expecting our samples to fully capture all interactions (Strydom *et al.* 2021). As a
331 result, better models for predicting interactions are needed for interaction networks. This includes
332 explicitly accounting for observation error (Johnson & Larremore 2021)—certain classes of models have
333 been used to reflect hidden states which account for detection error in occupancy modeling (Joseph 2020),
334 and could be integrated in the predictive models of interactions in the future.

335 This work has several practical consequences for the design of interaction samples. Simulating the process
336 of observation could be a powerful tool for estimating the sampling effort required by a study that takes
337 relative abundance into account, and provides a null baseline for expected FNR. It is necessary to take the
338 size of the species pool into account when deciding how many total samples is sufficient for an
339 “acceptable” FNR (fig. 2(C & D)). Further the spatial and temporal turnover of interactions means any
340 approach to sampling prioritization must be spatiotemporal. We demonstrated earlier that observed
341 negatives outside of the range of both species aren’t informative, and therefore using species distribution
342 models could aid in this spatial prioritization of sampling sites.

343 We also should address the impact of false-negatives on the inference of process and causality in
344 community ecology. We demonstrated that in model food webs, false-negatives do not impact the measure

of total trophic levels until very high FNR (figure fig. 5(C)), although we cannot generalize this further to other properties. This has immediate practical concern for how we design what taxa to sample—does it matter if the sampled network is fully connected? It has been shown that the stability of subnetworks can be used to infer the stability of the metaweb paper beyond a threshold of samples (Song *et al.* 2022b). But does this extend to other network properties? And how can we be sure we are at the threshold at which we can be confident our sample characterizes the whole system? We suggest that modeling observation error like we have done here can address these questions and aid in the design of samples of species interactions. To try and sample to avoid all false-negatives is a fool’s errand. Species ranges overlap to form mosaics, which themselves are often changing in time. Communities and networks don’t end in space, and the interactions that connect species on the ‘periphery’ of a given network to species outside the spatial extent of a given sample will inevitably appear as false-negatives in practical samples. The goal should instead be to sample a system enough to have a statistically robust estimate of the current state and empirical change over time of an ecological community at a given spatial extent and temporal resolution, and to determine what the sampling effort required prior to sampling.

Our work highlights the need for a quantitatively robust approach to sampling design, both for interactions (Jordano 2016) and all other aspects of biodiversity (Carlson *et al.* 2020). As anthropogenic forces create rapid shifts in our planet’s climate and biosphere, this is an imperative to maximize the amount of ecological information we get in our finite samples, and make our inferences and decisions based on this data as robust as possible. Where we choose to sample, and how often we choose to sample there, has strong impacts on the inferences we make from data. Incorporating a better understanding of sampling effort and bias to the design of biodiversity monitoring systems, and the inference and predictive models we apply to this data, is imperative in understanding how biodiversity is changing, and making actionable forecasts about the future of ecological interactions on our planet.

References

- Banville, F., Vissault, S. & Poisot, T. (2021). Mangal.jl and EcologicalNetworks.jl: Two complementary packages for analyzing ecological networks in Julia. *Journal of Open Source Software*, 6, 2721.
- Bascompte, J. & Jordano, P. (2007). Plant-Animal Mutualistic Networks: The Architecture of Biodiversity. *Annual Review of Ecology, Evolution, and Systematics*, 38, 567–593.

373 Becker, D.J., Albery, G.F., Sjodin, A.R., Poisot, T., Bergner, L.M., Dallas, T.A., *et al.* (2021). Optimizing
 374 predictive models to prioritize viral discovery in zoonotic reservoirs.

375 Bezanson, J., Edelman, A., Karpinski, S. & Shah, V.B. (2015). Julia: A Fresh Approach to Numerical
 376 Computing.

377 Blanchet, F.G., Cazelles, K. & Gravel, D. (2020). Co-occurrence is not evidence of ecological interactions.
 378 *Ecology Letters*, 23, 1050–1063.

379 Blaom, A.D., Kiraly, F., Lienart, T., Simillides, Y., Arenas, D. & Vollmer, S.J. (2020). MLJ: A Julia package
 380 for composable machine learning. *Journal of Open Source Software*, 5, 2704.

381 Boakes, E.H., Rout, T.M. & Collen, B. (2015). Inferring species extinction: The use of sighting records.
 382 *Methods in Ecology and Evolution*, 6, 678–687.

383 Canard, E., Mouquet, N., Marescot, L., Gaston, K.J., Gravel, D. & Mouillot, D. (2012). Emergence of
 384 Structural Patterns in Neutral Trophic Networks. *PLOS ONE*, 7, e38295.

385 CaraDonna, P.J., Petry, W.K., Brennan, R.M., Cunningham, J.L., Bronstein, J.L., Waser, N.M., *et al.* (2017).
 386 Interaction rewiring and the rapid turnover of plantpollinator networks. *Ecology Letters*, 20, 385–394.

387 Carlson, C.J., Dallas, T.A., Alexander, L.W., Phelan, A.L. & Phillips, A.J. (2020). What would it take to
 388 describe the global diversity of parasites? *Proceedings of the Royal Society B: Biological Sciences*, 287,
 389 20201841.

390 Cazelles, K., Araújo, M.B., Mouquet, N. & Gravel, D. (2016). A theory for species co-occurrence in
 391 interaction networks. *Theoretical Ecology*, 9, 39–48.

392 Closs, G.P. & Lake, P.S. (1994). Spatial and Temporal Variation in the Structure of an Intermittent-Stream
 393 Food Web. *Ecological Monographs*, 64, 1–21.

394 de Aguiar, M.A.M., Newman, E.A., Pires, M.M., Yeakel, J.D., Boettiger, C., Burkle, L.A., *et al.* (2019).
 395 Revealing biases in the sampling of ecological interaction networks. *PeerJ*, 7, e7566.

396 Gauzens, B., Legendre, S., Lazzaro, X. & Lacroix, G. (2013). Food-web aggregation, methodological and
 397 functional issues. *Oikos*, 122, 1606–1615.

398 Giacomuzzo, E. & Jordán, F. (2021). Food web aggregation: Effects on key positions. *Oikos*, 130,
 399 2170–2181.

400 Griffiths, D. (1998). Sampling effort, regression method, and the shape and slope of sizeabundance
 401 relations. *Journal of Animal Ecology*, 67, 795–804.

402 Hadfield, J.D., Krasnov, B.R., Poulin, R. & Nakagawa, S. (2014). A Tale of Two Phylogenies: Comparative
 403 Analyses of Ecological Interactions. *The American Naturalist*, 183, 174–187.

404 Havens, K. (1992). Scale and Structure in Natural Food Webs. *Science*, 257, 1107–1109.

405 Johnson, E.K. & Larremore, D.B. (2021). Bayesian estimation of population size and overlap from random
 406 subsamples.

407 Jordano, P. (2016). Sampling networks of ecological interactions. *Functional Ecology*, 30, 1883–1893.

408 Joseph, M.B. (2020). Neural hierarchical models of ecological populations. *Ecology Letters*, 23, 734–747.

409 Kenall, A., Harold, S. & Foote, C. (2014). An open future for ecological and evolutionary data? *BMC*
 410 *Evolutionary Biology*, 14, 66.

411 Khoshraftar, S. & An, A. (2022). A Survey on Graph Representation Learning Methods.

412 Koleff, P., Gaston, K.J. & Lennon, J.J. (2003). Measuring beta diversity for presenceabsence data. *Journal*
 413 *of Animal Ecology*, 72, 367–382.

414 Kopelke, J.-P., Nyman, T., Cazelles, K., Gravel, D., Vissault, S. & Roslin, T. (2017). Food-web structure of
 415 willow-galling sawflies and their natural enemies across Europe. *Ecology*, 98, 1730–1730.

416 Li, M., Liu, R.-R., Lü, L., Hu, M.-B., Xu, S. & Zhang, Y.-C. (2021). Percolation on complex networks:
 417 Theory and application. *Physics Reports*, Percolation on complex networks: Theory and application,
 418 907, 1–68.

419 MacDonald, A.A.M., Banville, F. & Poisot, T. (2020). Revisiting the Links-Species Scaling Relationship in
 420 Food Webs. *Patterns*, 1.

421 Makiola, A., Compson, Z.G., Baird, D.J., Barnes, M.A., Boerlijst, S.P., Bouchez, A., *et al.* (2020). Key
 422 Questions for Next-Generation Biomonitoring. *Frontiers in Environmental Science*, 7.

423 Martinez, N.D., Hawkins, B.A., Dawah, H.A. & Feifarek, B.P. (1999). Effects of Sampling Effort on
 424 Characterization of Food-Web Structure. *Ecology*, 80, 1044–1055.

425 McLeod, A., Leroux, S.J., Gravel, D., Chu, C., Cirtwill, A.R., Fortin, M.-J., *et al.* (2021). Sampling and
 426 asymptotic network properties of spatial multi-trophic networks. *Oikos*, 130, 2250–2259.

427 Moore, A.L. & McCarthy, M.A. (2016). Optimizing ecological survey effort over space and time. *Methods*
 428 *in Ecology and Evolution*, 7, 891–899.

429 Niedballa, J., Wilting, A., Sollmann, R., Hofer, H. & Courtiol, A. (2019). Assessing analytical methods for
 430 detecting spatiotemporal interactions between species from camera trapping data. *Remote Sensing in*
 431 *Ecology and Conservation*, 5, 272–285.

432 Paine, R.T. (1988). Road Maps of Interactions or Grist for Theoretical Development? *Ecology*, 69,
 433 1648–1654.

434 Poisot, T. (2022). Guidelines for the prediction of species interactions through binary classification.

435 Poisot, T., Bergeron, G., Cazelles, K., Dallas, T., Gravel, D., MacDonald, A., *et al.* (2021). Global knowledge
 436 gaps in species interaction networks data. *Journal of Biogeography*, 48, 1552–1563.

437 Poisot, T., Ouellet, M.-A., Mollentze, N., Farrell, M.J., Becker, D.J., Brierly, L., *et al.* (2022). Network
 438 embedding unveils the hidden interactions in the mammalian virome.

439 Poisot, T., Stouffer, D.B. & Gravel, D. (2015). Beyond species: Why ecological interaction networks vary
 440 through space and time. *Oikos*, 124, 243–251.

441 Ponisio, L.C., Gaiarsa, M.P. & Kremen, C. (2017). Opportunistic attachment assembles plantpollinator
 442 networks. *Ecology Letters*, 20, 1261–1272.

443 Savage, V.M., Gillooly, J.F., Brown, J.H., West, G.B. & Charnov, E.L. (2004). Effects of Body Size and
 444 Temperature on Population Growth. *The American Naturalist*, 163, 429–441.

445 Song, C., Simmons, B.I., Fortin, M.-J. & Gonzalez, A. (2022a). Generalism drives abundance: A
 446 computational causal discovery approach. *PLOS Computational Biology*, 18, e1010302.

447 Song, C., Simmons, B.I., Fortin, M.-J., Gonzalez, A., Kaiser-Bunbury, C.N. & Saavedra, S. (2022b). Rapid
 448 monitoring for ecological persistence.

449 Stephenson, P. (2020). Technological advances in biodiversity monitoring: Applicability, opportunities
 450 and challenges. *Current Opinion in Environmental Sustainability*, Open issue 2020 part A: Technology
 451 Innovations and Environmental Sustainability in the Anthropocene, 45, 36–41.

452 Stock, M., Poisot, T., Waegeman, W. & De Baets, B. (2017). Linear filtering reveals false negatives in
 453 species interaction data. *Scientific Reports*, 7, 45908.

454 Strydom, T., Catchen, M.D., Banville, F., Caron, D., Dansereau, G., Desjardins-Proulx, P., *et al.* (2021). A
 455 roadmap towards predicting species interaction networks (across space and time). *Philosophical*
 456 *Transactions of the Royal Society B: Biological Sciences*, 376, 20210063.

457 Thompson, P.L. & Gonzalez, A. (2017). Dispersal governs the reorganization of ecological networks under
 458 environmental change. *Nature Ecology & Evolution*, 1, 1–8.

459 Thompson, R.M. & Townsend, C.R. (2000). Is resolution the solution?: The effect of taxonomic resolution
 460 on the calculated properties of three stream food webs. *Freshwater Biology*, 44, 413–422.

461 Volkov, I., Banavar, J.R., Hubbell, S.P. & Maritan, A. (2003). Neutral theory and relative species abundance
 462 in ecology. *Nature*, 424, 1035–1037.

463 Walther, B.A., Cotgreave, P., Price, R.D., Gregory, R.D. & Clayton, D.H. (1995). Sampling Effort and
 464 Parasite Species Richness. *Parasitology Today*, 11, 306–310.

465 Williams, R.J. & Martinez, N.D. (2000). Simple rules yield complex food webs. *Nature*, 404, 180–183.

466 Willott, S.j. (2001). Species accumulation curves and the measure of sampling effort. *Journal of Applied*
 467 *Ecology*, 38, 484–486.

468 Young, J.-G., Valdovinos, F.S. & Newman, M.E.J. (2021). Reconstruction of plantpollinator networks from
 469 observational data. *Nature Communications*, 12, 3911.

470 Zhang, S., Tong, H., Xu, J. & Maciejewski, R. (2019). Graph convolutional networks: A comprehensive
 471 review. *Computational Social Networks*, 6, 11.

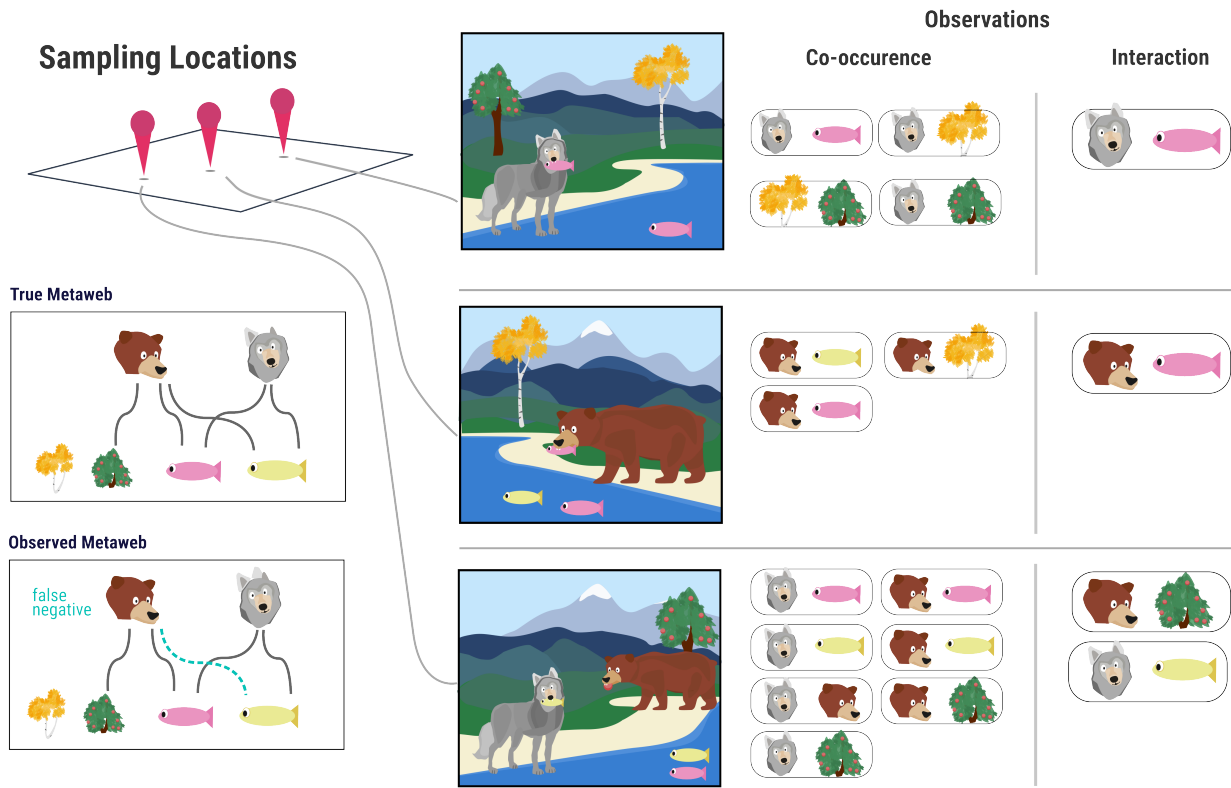


Figure 1: This conceptual example considers a sample of the trophic community of bears, wolves, salmon (pink fish), pike (yellow fish), berry trees, and aspen trees. The true metaweb (all realized interactions across the entire spatial extent) is shown on the left. In the center is what a hypothetical ecologist samples at each site. Notice that although bears are observed co-occurring with both salmon and pike, there was never a direct observation of bears eating pike, even though they actually do. Therefore, this interaction between bears and pike is a false negative.

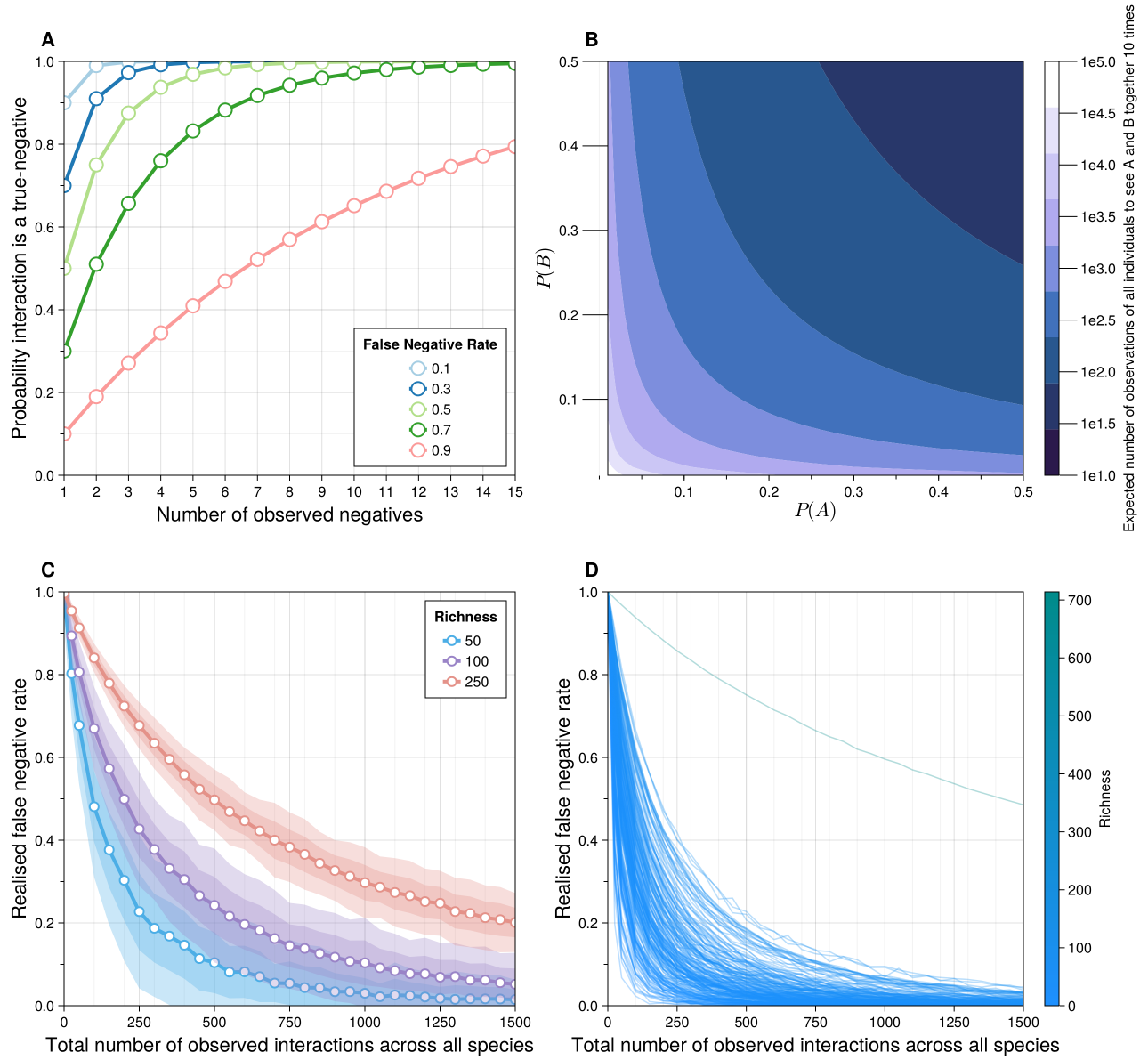


Figure 2: **(A)** The probability that an observed interaction is a true negative (y-axis) given how many times it has been sampled as a non-interaction (x-axis). Each color reflects a different value of p_{fn} , the false-negative rate (FNR)—this is effectively the cdf of the geometric distribution. **(B)** The expected number of total observations needed (colors) to observe 10 co-occurrences between a species with relative abundance $P(A)$ (x-axis) and a second species with relative abundance $P(Y)$. **(C)**: False negative rate (y-axis) as a function of total sampling effort (x-axis) and network size, computed using the method described above. For 500 independent draws from the niche model (Williams & Martinez (2000)) at varying levels of species richness (colors) with connectance drawn according to the flexible-links model (MacDonald *et al.* (2020)) as described in the main text. For each draw from the niche model, 200 sets of 1500 observations are simulated, for which each the mean false negative rate at each observation-step is computed. Means denoted with points, with 1 in the first shade and 2 in the second. **(D)**: Same as **(C)**, except using empirical food webs from Mangal database, where richness. The outlier on **(D)** is a 714 species food-web.

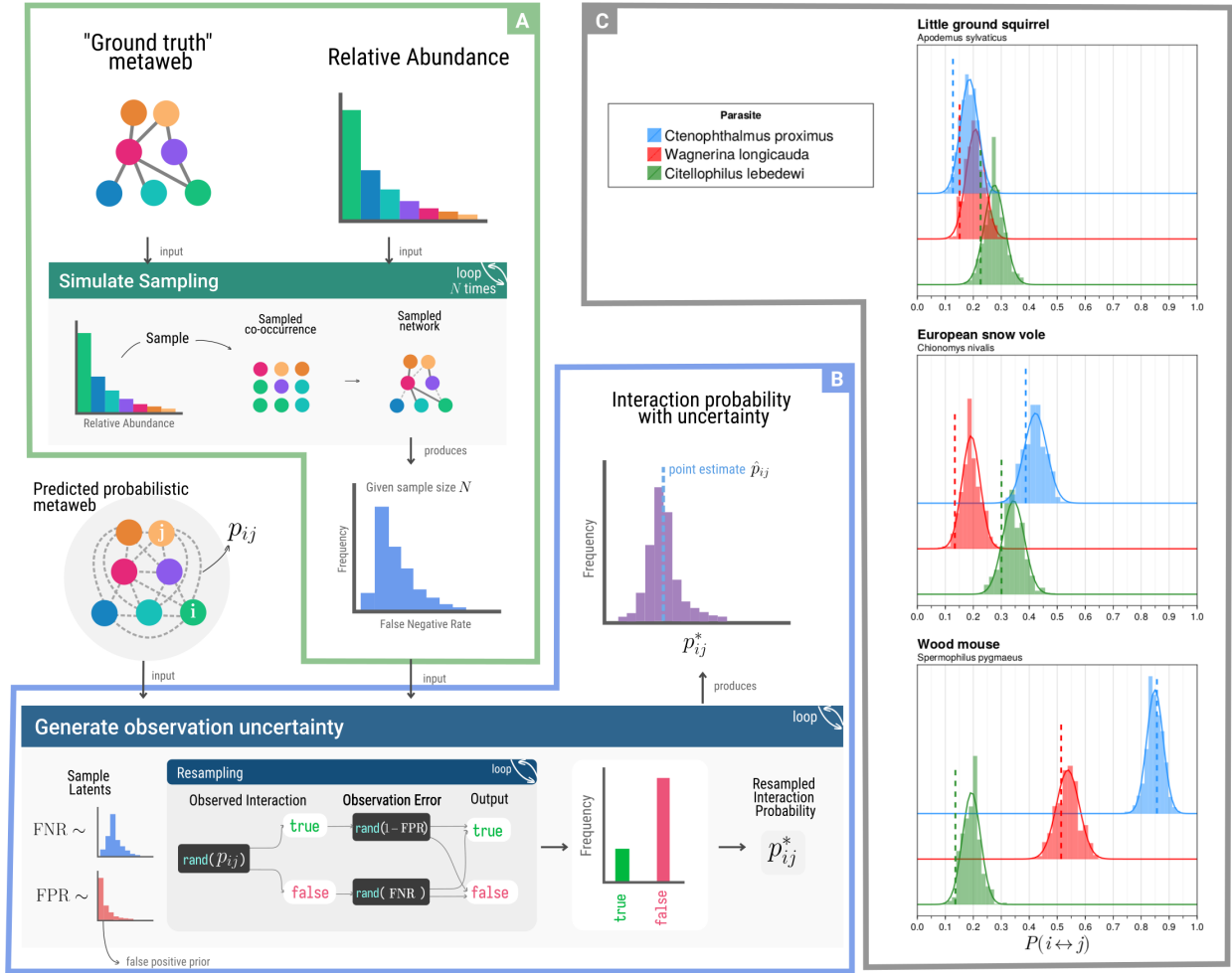


Figure 3: (A) The process for estimating the false-negative rate (FNR) for an interaction dataset consisting of N total observed interactions. (B) The method for resampling interaction probability based on estimates of false-negative and false-positive rates. (C) The method for interaction probability resampling applied to three mammals and three parasites from the Hadfield *et al.* (2014) dataset.

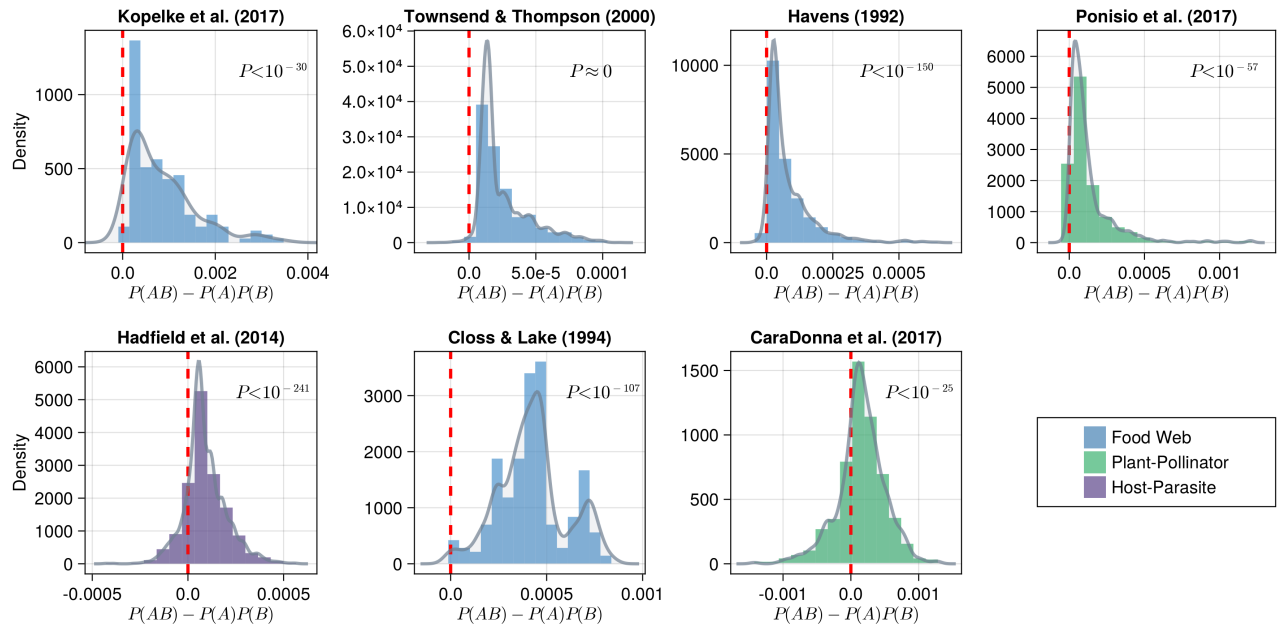


Figure 4: The difference between joint-probability of co-occurrence ($P(AB)$) and expected probability of co-occurrence under independence ($P(A)P(B)$) for interacting species for each dataset. The red-dashed line indicates 0 (no association). Each histogram represents a density, meaning the area of the entire curve sums to 1. The continuous density estimate (computed using local smoothing) is shown in grey. The p-value on each plot is the result of a one-sided t-test comparing the mean of each distribution to 0.



Figure 5: **(A)** The area-under the receiver-operator curve (ROC-AUC) and **(B)** The area-under the precision-recall curve (PR-AUC; right) for each different predictive model (colors/shapes) across a spectrum of the proportion of added false negatives (x-axis). **(C)** The mean trophic-level of all species in a network generated with the niche model across different species richnesses (colors). For each value of the FNR, the mean trophic level was computed across 50 replicates. The shaded region for each line is one standard-deviation across those replicates.